Co-support compound formation in titania-supported cobalt catalyst

Bunjerd Jongsomjit[a,*], Chitlada Sakdamnuson[a], James G. Goodwin Jr[b], and Piyasan Praserthdam[a]

[a]*Center of Excellence on Catalysis and Catalytic Reaction Engineering, Department of Chemical Engineering, Faculty of Engineering, Chulalongkorn University, Bangkok 10330, Thailand*

[b]*Department of Chemical Engineering, Clemson University, Clemson, SC 29634, USA*

Received 2 December 2003; accepted 25 February 2004

Co-support compound formation (Co-SCF) in Co/TiO_2 was found during standard reduction resulting in a lower reducibility of the catalyst. The compound formed is considered to be non-reducible at temperatures <800 °C during TPR and different from $CoTiO_3$. The characteristics of Co-SCF were investigated using BET surface area, XRD, Raman spectroscopy, SEM/EDX, and TPR.

KEY WORDS: supported catalyst; cobalt catalyst; cobalt-support compound; titania support; Co/TiO_2; reducibility; CO hydrogenation.

1. Introduction

In Fischer–Tropsch synthesis (FTS), supported cobalt catalysts are preferred because of their high activity for FTS based on natural gas [1], high selectivity to linear long-chain hydrocarbons and low activity for the water–gas shift (WGS) reaction [2,3]. However, compound formation between cobalt and the supports can occur during the catalyst activation and/or reaction conditions resulting in irreversible catalyst deactivation [4–6].

Besides alumina (Al_2O_3) and silica (SiO_2), titania (TiO_2) has been widely studied as the support for cobalt catalysts by many authors [7–20], especially for the application of FTS in a continuously stirred tank reactor (CSTR) [11,15]. It was reported that Co-SCF in SiO_2 [21] and Al_2O_3 [4–6,22] can occur during standard reduction and resulted in a lower degree of reduction. However, titania was the first support where strong metal support interaction was observed [19]. In the present research, the nature of Co-SCF in titania-supported cobalt catalyst and its effect on the characteristics of the catalysts were the main focus. In this study, the Co/TiO_2 catalyst was prepared, pretreated under various conditions, and characterized using BET surface area, XRD, TPR, SEM/EDX, and Raman spectroscopy to identify the nature of compounds formed. The main objectives of this research were to develop a better understanding of Co-SCF in titania-supported cobalt catalyst and to better identify the compounds formed. Based on information obtained from the present research, the strategies to minimize such a compound formation can be further developed.

2. Experimental

2.1. *Catalyst preparation*

A 20 wt% of Co/TiO_2 was prepared by the incipient wetness impregnation. A designed amount of cobalt nitrate $[Co(NO_3) \cdot 6H_2O]$ was dissolved in deionized water and then impregnated onto TiO_2 (anatase form calcined at 600 °C obtained from Ishihara Sangyo, Japan). The catalyst precursor was dried at 110 °C for 12 h and calcined in air at 500 °C for 4 h.

2.2. *Catalyst pretreatments*

Standard reduction of the calcined catalyst was conducted in a fixed-bed flow reactor under differential conditions at 1 atm using a temperature ramp from ambient to 350 °C at 1 °C/min and holding at 350 °C for 10 h in a gas flow having a space velocity of 16,000 h^{-1} and consisting of H_2 or mixtures of H_2 and water vapor (5–10 vol%). The high space velocity of the H_2 flow when water vapor was not added insured that the partial pressure of water vapor in the catalyst bed produced by cobalt oxide reduction would be essentially zero in that case. The reduced catalyst was then passivated at room temperature with air for 30 min.

2.3. *Catalyst nomenclature*

The nomenclature used for the catalyst samples in this study is following:

- Co–C: the calcined catalyst sample
- Co–RW0: the calcined catalyst sample reduced in H_2
- Co–RW5: the calcined catalyst sample reduced in a mixture of H_2 with 5 vol% water vapor added during reduction
- Co–RW10: the calcined catalyst sample reduced in a mixture of H_2 with 10 vol% water vapor added during reduction

---

[*] To whom correspondence should be addressed.
E-mail: bunjerd.j@chula.ac.th

1011-372X/04/0500–0209/0 © 2004 Plenum Publishing Corporation

2.4. *Catalyst characterization*

2.4.1. *BET surface area*

BET surface area of the samples after various pretreatments was performed to determine if the total surface area changes upon the various pretreatment conditions. It was determined using N_2 adsorption at 77 K in a Micromeritics ASAP 2010.

2.4.2. *X-ray diffraction*

XRD was performed to determine the bulk crystalline phases of catalyst following different pretreatment conditions. It was conducted using a SIEMENS D–5000 X-ray diffractometer with CuK_α ($\lambda = 1.54439$ Å). The spectra were scanned at a rate of 2.4 °/min in the range $2\theta = 20–80°$.

2.4.3. *Scanning electron microscopy and energy dispersive X-ray spectroscopy*

SEM and EDX were used to determine the catalyst morphologies and elemental distribution throughout the catalyst granules, respectively. The SEM of JEOL mode JSM–5800LV was applied. EDX was performed using Link Isis series 300 program.

2.4.4. *Raman spectroscopy*

The Raman spectra of the samples were collected by projecting a continuous wave laser of argon ion (Ar^+) green (514.532 nm) through the samples exposed to air at room temperature. A scanning range of 100–1000 cm^{-1} with a resolution of 2 cm^{-1} was applied. The data were analyzed using the Renishaw WiRE (Windows-based Raman Environment) software, which allows Raman spectra to be captured, calibrated, and analyzed using system 2000 functionality via Galactic GRAMS interface with global imaging capacity.

2.4.5. *Temperature-programmed reduction*

TPR was used to determine the reduction behaviors and reducibilities of the samples. It was carried out using 50 mg of a sample and a temperature ramp from 35 to 800 °C at 5 °C/min. The carrier gas was 5% H_2 in Ar. A cold trap was placed before the detector to remove water produced during the reaction. A thermal conductivity detector (TCD) was used to determine the amount of H_2 consumed during TPR. The H_2 consumption was calibrated using TPR of Ag_2O at the same conditions. The reduced samples were recalcined at the original calcination conditions prior to performing TPR. The calculation of reducibilities was described elsewhere [4–6,21,22,23].

2.5. *Reaction*

CO hydrogenation ($H_2/CO = 10/1$) was performed to determine the overall activity of the catalyst samples reduced at various conditions. Hydrogenation of CO was carried out at 220 °C and 1 atm. A flow rate of $H_2/CO/He = 20/2/8$ cc/min in a fixed-bed flow reactor under differential conditions was used. A relatively high H_2/CO ratio was used to minimize deactivation due to carbon deposition during reaction. Typically, 20 mg of a catalyst sample was re-reduced *in situ* in flowing H_2 (30 cc/min) at 350 °C for 10 h prior to the reaction. Reactor effluent samples were taken at 1 h intervals and analyzed by GC. In all cases, steadystate was reached within 5 h.

3. Results and discussion

3.1. *Evidence of Co-SCF in Co/TiO_2 catalyst*

It can be observed that Co-SCF in Co/TiO_2 essentially occurred during standard reduction resulting in lower reducibilities of the reduced samples during TPR at temperatures 35–800 °C as shown in table 1. The reducibilities ranged from 92% to 64% upon the various pretreatments of catalyst samples. Essentially, TPR of the TiO_2 support only (table 1) was also conducted at the same condition and no hydrogen consumption was detected. It should be noted that the loss in the degree of reduction was attributed to the compound formation of cobalt and the titania support. The suggested conceptual diagram of reducibility loss during standard reduction is illustrated in figure 1. First, when performing TPR on a fresh calcined sample, the reducibility gain was 92%. However, when the calcined sample was reduced with and without water vapor addition (5–10 vol%) during reduction, then recalcined it back to the oxide form prior to performing TPR, the reducibilities obviously decreased. The reducibilities loss during the reduction process were found to be in the range of 22–28% indicating the non-reducible (at temperatures < 800 °C) "Co-titanate" compound formed. The term "Co-titanate" is used here to refer to the surface compound formed during standard reduction of cobalt and the titania support.

It should be mentioned that a decrease in the degree of reduction of reduced samples slightly changed upon

Table 1
Reducibilities and surface areas of samples after various pretreatments

Sample	Reduction gas mixture (P_{H2}/P_{H2O})	Reducibility (%) during TPR at 35–800 °C[a,b]	Surface area (m^2/g)[b]
TiO_2	–	–	70
Co–C	–	92	52
Co–RW0	1/0	70	49
Co–RW5	0.95/0.05	68	46
Co–RW10	0.90/0.10	64	46

[a] The reduced samples were recalcined at the original calcination conditions prior to performing TPR.

[b] Measurement error is ±5%.

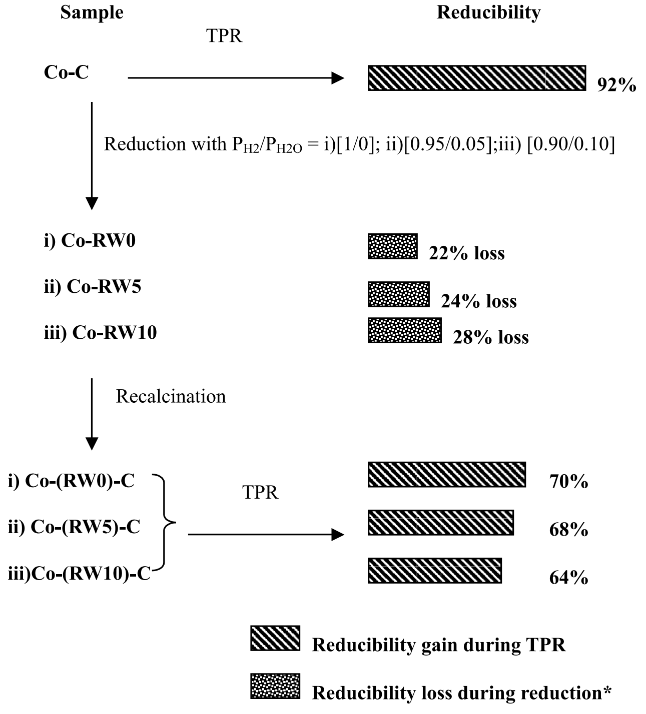

* The difference in reducibility gain from a fresh calcined sample and the reducibility gain from a reduced and recalcined sample.

Figure 1. Suggested conceptual diagram for the reducibility loss during reduction process.

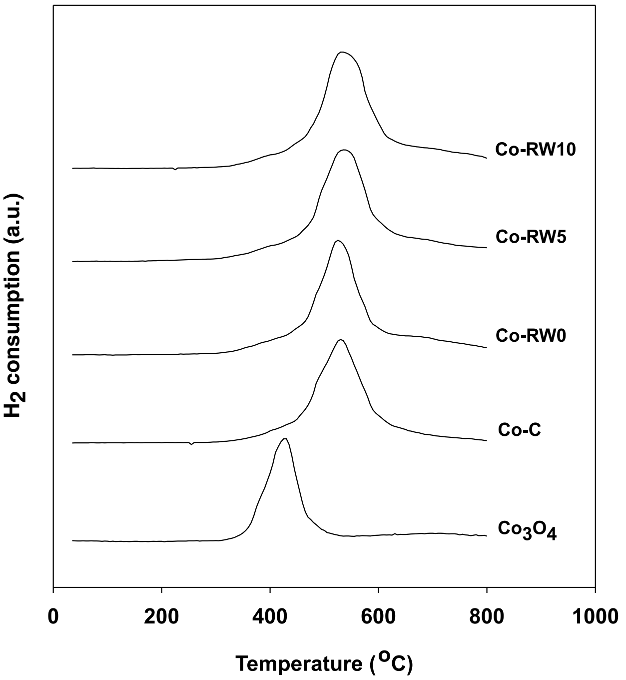

Figure 2. TPR profiles of bulk Co_3O_4 and the catalyst samples after various pretreatment conditions.

increasing the partial pressures of water vapor during the reduction process. Zhang *et al.* [22] investigated the reducibilities of CoRu/γ-Al_2O_3 during standard reduction and TPR in the presence of added water vapor. They reported that water has a significant effect on the reduction behavior of CoRu/γ-Al_2O_3. It was suggested that water vapor present during reduction leads to a decrease in the degree of reduction of the cobalt perhaps in two ways: (i) inhibition of the reduction of well-dispersed CoO interacting with the alumina support, possibly by increasing the cobalt–alumina interaction, and (ii) facilitation of the migration of cobalt ions into probable tetrahedral sites of γ-Al_2O_3 to form a non-reducible (at temperatures < 900 °C) spinel. However, considering the Co-SCF in Co/TiO_2, the effect of water vapor added during standard reduction was essentially less pronounced compared to that on the alumina support. The only slight effect of water vapor on Co-SCF in Co/TiO_2 is also listed in table 1 indicating that the reducibilities of the reduced samples only slightly decreased within experimental error when water vapor (5–10 vol%) was added during standard reduction. Besides the reducibility measurement, TPR also provides information on the reduction behaviors of the catalyst samples pretreated under various conditions.

TPR profiles of bulk Co_3O_4 and the catalyst samples after various pretreatment conditions are shown in figure 2. Only one strong reduction peak can be observed for bulk Co_3O_4 and all the samples regardless of various pretreatment conditions used. This peak can be assigned to the overlap of two-step reduction of Co_3O_4 to CoO and then to Co^0 [22,24,25]. Upon the TPR conditions, the two reduction peaks based on the two-step reduction may or may not be observed. The TPR profile of the titiania support (not shown) showed no reduction peak. There was only one reduction peak located at ca. 370–620 °C (max. at 520 °C) for the calcined sample (Co–C) indicated that no residual cobalt nitrates remain on the calcined sample of Co/TiO_2 upon the calcination condition used in this study. In some cases, the peak of the decomposition of cobalt nitrates during TPR of supported cobalt catalysts can be observed at temperatures between 200 and 300 °C, especially with silica and alumina supports [4–6,23,26,27]. However, prolonged calcination or reduction and recalcination results in complete decomposition of any cobalt nitrates present [23].

TPR profiles of all reduced samples were also similar exhibiting only one reduction peak as shown in figure 2. TPR peak located at ca. 400–620 °C (max. at 520 °C) for Co-RW0 sample was slightly shifted about 10 °C higher when the partial pressure of water vapor was increased during reduction indicating slightly stronger interaction between cobalt and titania support. However, the much stronger interaction between cobalt and the supports such as silica and alumina can be usually observed leading to an observation of two separated peaks during TPR of the reduced and recalcined samples [4–6,21,23]. The higher temperature reduction peak can be assigned to the reduction of cobalt strongly interacting with the supports, i.e. Co_XO_Y–Al_2O_3 and Co_XO_Y–SiO_2, which can not be observed in the reduced and recalcined Co/TiO_2 catalyst. Based on the TPR results, it should be noted that a degree of reduction of the reduced Co/TiO_2 catalyst was found to decrease during standard reduction due to "Co-titanate" formed. However, the reduction behaviors of samples reduced in various conditions were similar upon the TPR measurement conditions used in this study. This can be concluded that "Co-titanate" formed in a Co/TiO_2 catalyst resulted in only a decrease in the reducibility without changing the reduction behaviors of it. The effect of partial pressures of water vapor during reduction on the formation of "Co-titanate" seemed to be less pronounced.

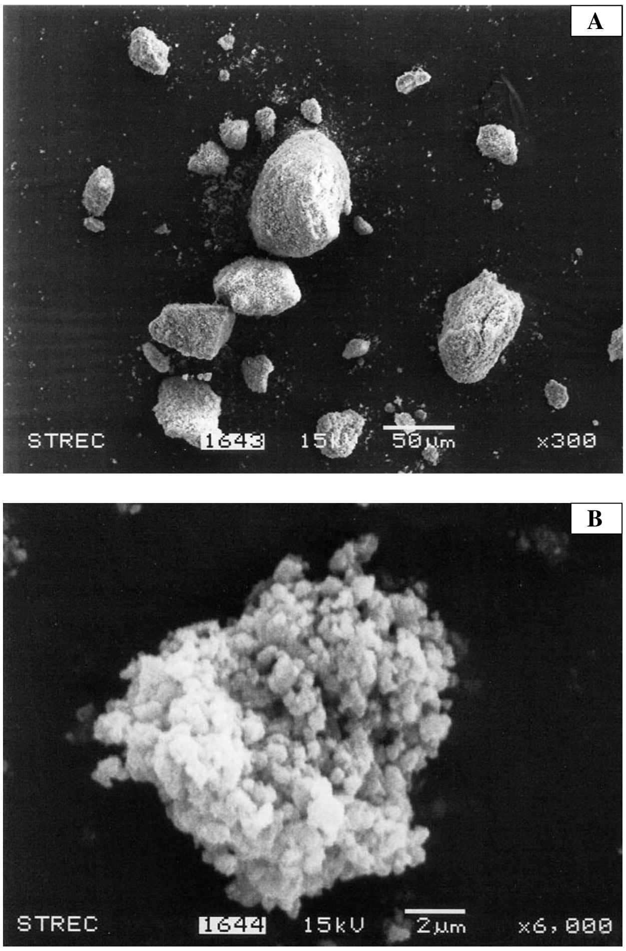

Figure 3. SEM micrographs of Co-RW10 catalyst granule at the external surface; (a) at 300× magnification and (b) at 6000× magnification.

3.2. *Characteristics of "Co-titanate"*

In order to identify the characteristics of "Co-titanate" formed during reduction, several characterization techniques were conducted. BET surface areas of TiO_2 and the catalyst samples after various pretreatments are also shown in table 1. BET surface areas of samples were slightly less than the titania (anatase form) support (70 m^2/g). Since all surface areas of the samples in this study ranged between 46 and 52 m^2/g, there was no significant change in surface areas after the various pretreatments within experimental errors. This indicated that "Co-titanate" formed did not cause any change in surface areas of the catalyst.

SEM and EDX were performed to study the morphologies of the catalyst samples and elemental distributions of the catalyst samples, respectively. There was no significant change in morphologies of catalyst samples due to the "Co-titanate" formed. By observation on the external surface of the catalyst granules, cobalt patches (the term "patches" is used to refer to the entities rich in cobalt supported on the catalyst granules) can be seen all over the external surface of samples. In general, all of them were similar regardless of the pretreatment conditions used. The typical morphology in an external area of catalyst granules with different magnification for Co-RW10 is shown in figure 3. It can be observed that cobalt patches (white spots) were well distributed all over the external surface of catalyst granules. The elemental distributions can be clearly seen by EDX. Figure 4 shows the typical elemental distribution for a cross section of a granule of Co-RW10. The distribution of cobalt was well dispersed throughout the catalyst granule as also seen by SEM. Thus, there was no significant change in catalyst morphologies and elemental distribution upon the formation of "Co-titanate".

The bulk crystalline phases of samples were determined using XRD. XRD patterns of TiO_2, $CoTiO_3$ (synthesized, based on reference [28]) and catalyst samples after various pretreatments are shown in figure 5. XRD patterns of TiO_2 showed strong diffraction peaks at 26°, 37°, 48°, 55°, 56°, 62°, 69°, 71° and 75° indicating the TiO_2 in the anatase form. After calcination, the diffraction peaks of Co_3O_4 at 36°, 46°, and 65° can be observed. Apparently, the relative intensity of those peaks is much lower compared to the TiO_2 peaks. To identify the XRD peaks of samples, XRD peaks of $CoTiO_3$ were also collected and it showed the diffraction peaks at 23°, 32°, 35°, 49°, 52°, 62° and 64° as also shown in figure 5. Kraum *et al.* [29] reported the observation for XRD peaks of $CoTiO_3$ phase along with Co_3O_4 on the calcined Co/TiO_2 catalyst using cobalt (III) acetyl acetonate as a precursor for cobalt. They suggested that the formation of $CoTiO_3$ by the use of cobalt (III) acetyl acetonate as a precursor can be attributed to the migration of cobalt ions into the support lattice, with the consecutive formation of titanate. However, based on differences in the cobalt precursor, the amounts of cobalt loading and the calcination condition used in the present study, the formation of $CoTiO_3$ was not observed in the calcined Co/TiO_2 catalyst. After reduction at various conditions and passivation, the diffraction peaks of CoO were

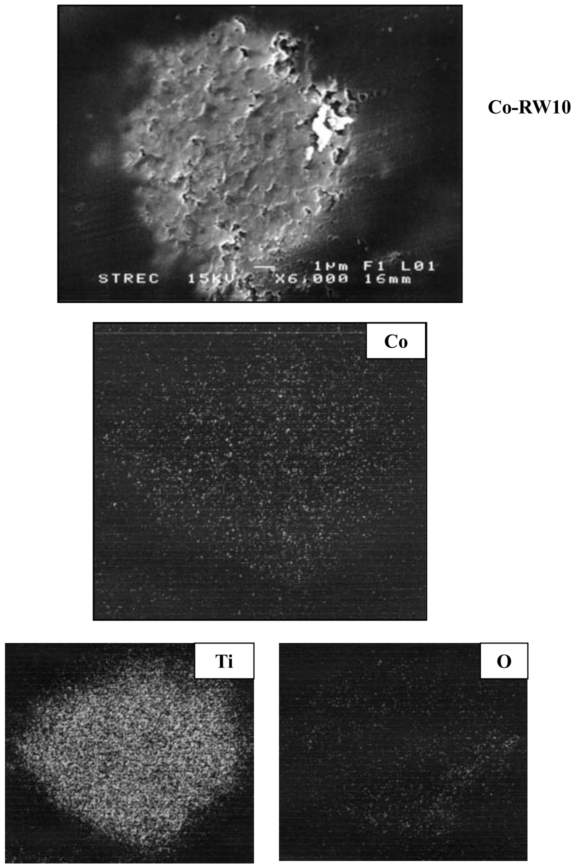

Figure 4. SEM micrograph and EDX mapping of Co-RW10 catalyst granule (cross section).

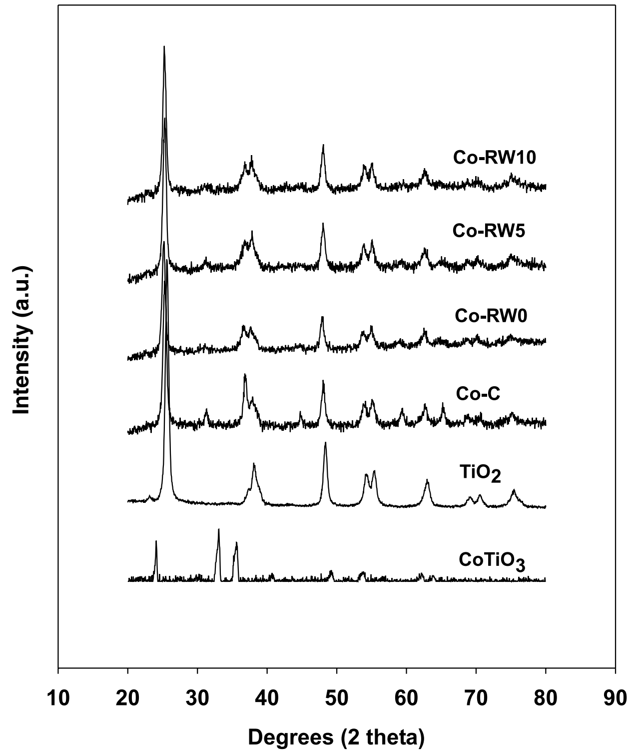

Figure 5. XRD patterns of TiO_2, $CoTiO_3$ and the catalyst samples after various pretreatment conditions.

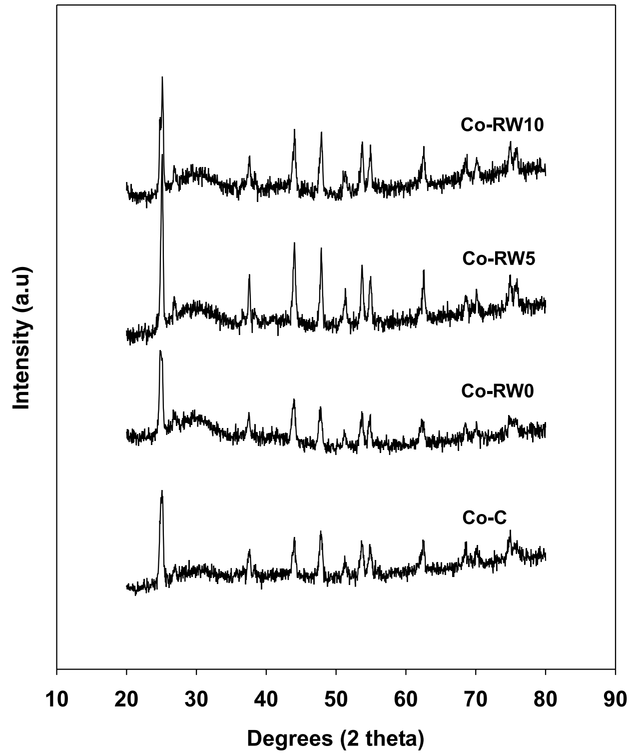

Figure 6. XRD patterns of the catalyst samples after TPR measurement up to 800 °C.

present at 37° and 63°. This indicated that Co_3O_4 in the calcined samples was reduced to highly dispersed cobalt metal and CoO during standard reduction at 350 °C. Any Co_3O_4 formed during passivation was present in only very thin surface layers and was consequently XRD invisible. No XRD peaks for "Co-titanate" formed were detected for any of the catalyst samples. In order to investigate the structure of non-reducible (at temperatures <800 °C during TPR) "Co-titanate", XRD was also conducted on the samples after performing TPR up to 800 °C. XRD patterns of samples after TPR measurement up to 800 °C are shown in figure 6. The similar trend as shown in figure 5 was found except for the observation of cobalt metal peaks at 44° and 52° due to sintering. No phase change, i.e from anatase to rutile form of TiO_2 was observed. XRD results revealed that the "Co-titanate" formed was in a highly dispersed form, thus, it is invisible in XRD after either standard reduction or TPR.

Raman spectra of TiO_2, CoO, Co_3O_4, $CoTiO_3$ and the catalyst samples after various pretreatments are shown in figure 7. To identify Raman bands of samples, the Raman spectra of Co_3O_4, CoO and $CoTiO_3$ were collected. The Raman bands of $CoTiO_3$ exhibited bands at 695, 604, 455, 382, 336 and 266 cm^{-1} which are similar to the ones reported by Brik *et al.* [30]. The strong Raman bands for TiO_2 were observed at 640, 514, and 397 cm^{-1} indicating the TiO_2 in its anatase form [9]. The Raman spectrum of the calcined sample exhibited Raman bands

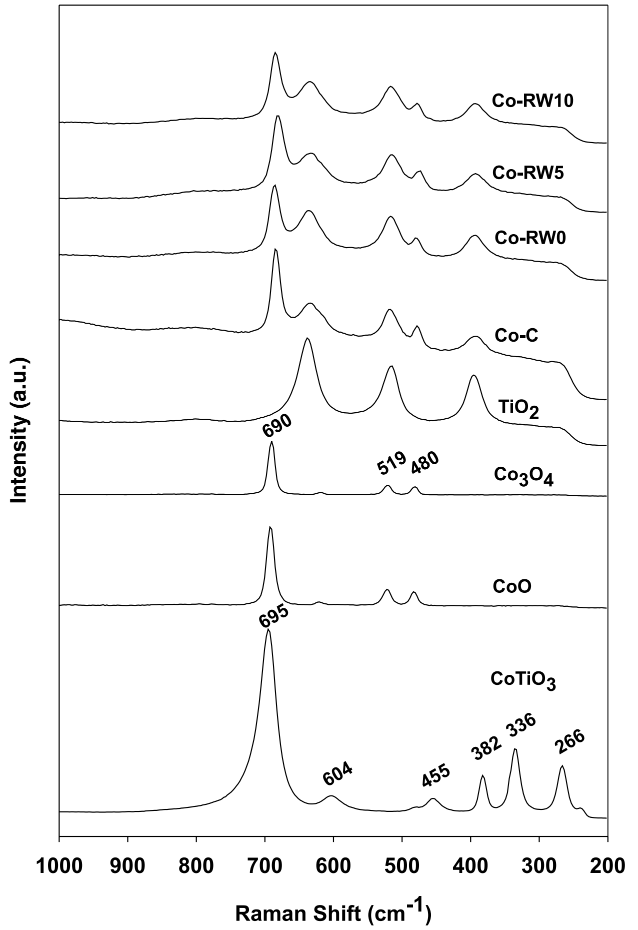

Figure 7. Raman spectra of TiO_2, Co_3O_4, CoO, $CoTiO_3$ and the catalyst samples after various pretreatment conditions.

at 640, 514, and 397 cm^{-1} as seen in those for TiO_2 including two shoulders at 690 and 480 cm^{-1}, assigned to Co_3O_4 [4–6]. Raman spectra of all reduced samples showed the Raman bands of TiO_2 support and the shoulders at 690 and 480 cm^{-1}. These can be assigned to Co_3O_4 present on catalyst surface rather than CoO (detected in the bulk by XRD) since Raman spectroscopy is more of surface technique [5]. This indicated that "Co-titanate" formed during reduction was different from $CoTiO_3$ and invisible in Raman spectroscopy. The invisible "Co-titanate" bands was probably caused by (i) its highly dispersed form and (ii) the Raman signals were hindered due to the highly strong Raman intensities of TiO_2 support. It was reported that reduced samples of Co/γ–Al_2O_3 at high partial pressure of water vapor during reduction exhibited the broad Raman bands between 400–700 cm^{-1} [4]. This was suggested that these broad Raman bands represent a surface cobalt compound related to cobalt strongly interacting with the alumina support as a "Co-aluminate". The identified "Co-alumiante" was suggested to be different from $CoAl_2O_4$ (spinel) due to being a non-stoichiometric surface "Co-aluminate" compound. This highly dispersed "Co-aluminate" may be formed, possibly by cobalt migration into the alumina matrix and was detectable using Raman spectroscopy, but not XRD. In addition, the alumina support itself does not exhibit any of Raman bands between 100 and 1000 cm^{-1}, thus, the Raman bands of "Co-aluminate" can be clearly detected. However, in the present study, the highly strong Raman intensities of the titania support may result in a hindrance of the Raman bands, if present, of the highly dispersed "Co-titanate" formed. Besides the strong signal of TiO_2, the signal of CoO and Co_3O_4 is likely to hinder the observation of surface "Co-titanate" as well. In order to eliminate that interference, we also conducted Raman spectroscopy on the reduced samples with a lesser degree of passivation and the Raman spectra of samples are shown in figure 8. It can be observed that the characteristic peaks of the reduced samples were similar to each other, but deviated from the characteristic peaks of Co_3O_4 as seen in figure 7. The Raman band of the reduced samples at 397 cm^{-1} of the TiO_2 became broader. This perhaps resulted from the overlap between the peaks of 397 cm^{-1} of the TiO_2 and 382 cm^{-1} of $CoTiO_3$ due to the formation of surface "Co-titanate". However, to elucidate all kinds of hindrances, rigorous surface techniques may be needed for further investigation. Nevertheless, Raman spectroscopy revealed that the "Co-titanate" formed was different from $CoTiO_3$ probably due to it also being non-stoichiometric (cobalt deficiency) surface "Co-titanate" compound.

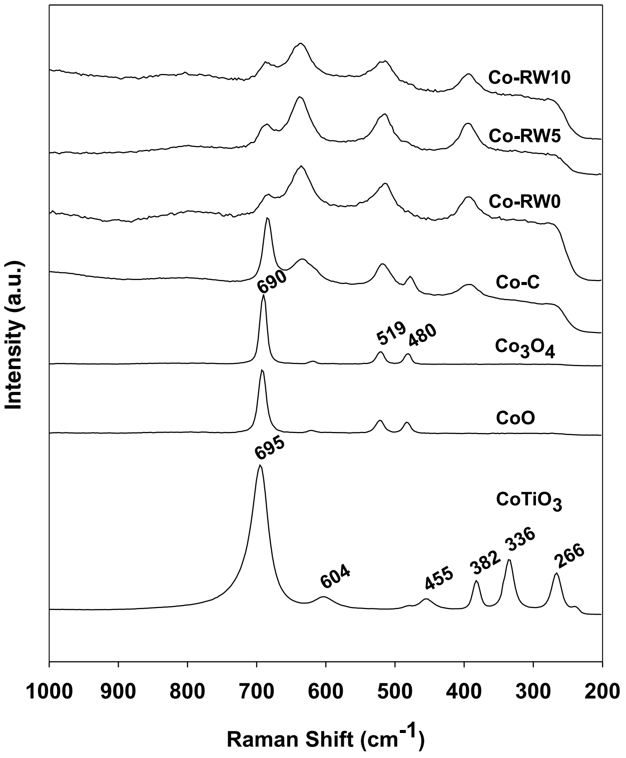

Figure 8. Raman spectra of Co_3O_4, CoO, $CoTiO_3$, the calcined sample and the reduced with a lesser degree of passivation samples.

CO hydrogenation was performed to determine the overall activity of the catalyst samples reduced at

Table 2
Reaction rate for CO hydrogenation on catalyst samples reduced at various conditions

Sample	CO conversion (%)[a]		Rate (μmol/gcat.s)[b]		CH_4 selectivity (%)	
	Initial[c]	SS[d]	Initial	SS	Initial	SS
Co–C	3.71	2.09	1.39	0.79	99	99
Co–RW0	1.53	0.73	0.58	0.27	99	99
Co–RW5	0.83	0.46	0.31	0.17	99	99
Co–RW10	0.34	0.08	0.13	0.03	98	98

[a] CO hydrogenation was carried out at 220 °C, 1.8 atm, and $H_2/CO/He = 20/2/8$ cc/min).
[b] Error ±5%.
[c] After 5 min of reaction.
[d] After 5 h of reaction.

various conditions. The results are shown in table 2. It indicated that the CO conversion ranged between 3.71 and 0.34% (initial) and 2.09 to 0.08% (steady state). The reaction rate ranged between 1.39 and 0.13 μmol/g cat.s (initial) and 0.79–0.03 μmol/g cat.s (steady). This suggested that the "Co-titanate" formed in the reduced samples resulted in decreased activities of catalyst. However, there was no significant difference in selectivity for any of samples based on reaction conditions used in this study.

4. Conclusions

We have shown that Co-support compound formation (Co-SCF) in titania-supported cobalt catalyst can occur during standard reduction resulting in a lower reducibility of catalyst. The compound of cobalt and titania formed referred as "Co-titanate" was considered to be non-reducible at temperatures < 800 °C. The "Co-titanate" formed resulted in a decrease in the degree of reduction without any significant change in the reduction behaviors. It was found that the partial pressures of water vapor during reduction probably had only a slight effect on an increase in the "Co-titanate" formation. Due to its highly dispersed form, it can not be detected by XRD. However, Raman spectroscopy revealed that this highly dispersed "Co-titanate" formed was likely to be different from $CoTiO_3$ and present as a non-stoichiometric surface "Co-titanate" compound. The "Co-titanate" formed also resulted in decreased activities of catalyst without any changes in selectivity.

Acknowledgments

We gratefully acknowledge the financial support by the National Research Council (NRC), the Thailand Research Fund (TRF) and TJTTP-JBIC. We would like to extend our thanks to the National Metal and Materials Technology Center (MTECH) for Raman spectroscopy analysis.

References

[1] H.P. Wither Jr., K.F. Eliezer and J.W. Michell, Ind. Eng. Chem. Res. 29 (1990) 1807.
[2] E. Iglesia, Appl. Catal. A 161 (1997) 59.
[3] R.C. Brady and R.J. Pettit, J. Am. Chem. Soc. 103 (1981) 1287.
[4] B. Jongsomjit, J. Panpranot and J.G. Goodwin Jr., J. Catal. 204 (2001) 98.
[5] B. Jongsomjit and J.G. Goodwin Jr., Catal. Today 77 (2002) 191
[6] B. Jongsomjit, J. Panpranot and J.G. Goodwin Jr., J. Catal. 205 (2003) 66.
[7] W.S. Epling, P.K. Cheekaamarla and A.M. Lane, Chem. Eng. J. 93 (2003) 61.
[8] A. Voβ, D. Borgmann and G. Wedler, J. Catal. 212 (2002) 10.
[9] Y. Brik, M. Kacimi, F. Bozon-Verduraz and M. Ziyad, J. Catal. 211 (2002) 470.
[10] D.J. Duvenhage and N.J. Coville, Appl. Catal. A 233 (2002) 63.
[11] J.L. Li, G. Jacobs, T. Das and B.H. Davis, Appl. Catal. A 233 (2002) 255.
[12] K. Nakaoka, K. Takanabe and K. Aika, Chem. Commun. 9 (2002) 1006.
[13] N.N. Madikizela and N.J. Coville, J. Mol. Catal. A-Chem. 181 (2002) 129.
[14] N.J. Coville and J.L. Li, Catal. Today 71 (2002) 403.
[15] J.L. Li, L.G. Xu, R. Keogh and B. Davis, Catal. Lett. 70 (2000) 127.
[16] D.G. Wei, J.G. Goodwin Jr., R. Oukaci and A.H. Singleton, Appl. Catal. A 210 (2001) 137.
[17] J.L. Li and N.J. Coville, Appl. Catal. A 208 (2001) 177.
[18] R. Zennaro, M. Tagliabue and C.H. Bartholomew, Catal. Today 58 (2000) 309.
[19] R. Riva, H. Miessuer, R. Vitali and G. Del Piero, Appl. Catal. A 196 (2000) 111.
[20] J.L. Li and N.J. Coville, Appl. Catal. A 181 (1999) 201.
[21] A. Kogelbauer, J.C. Weber and J.G. Goodwin Jr., Catal. Lett. 34 (1995) 269.
[22] Y. Zhang, D. Wei, S. Hammache and J.G. Goodwin Jr., J. Catal. 188 (1999) 281.
[23] A. Kogelbauer, J.G. Goodwin Jr. and R. Oukaci, J. Catal. 160 (1996) 125.
[24] D. Schanke, S. Vada, E.A. Blekkan, A. Hilmen, A. Hoff and A. Holmen, J. Catal. 156 (1995) 85.
[25] B.A. Sexton, A.E. Hughes and T.W. Turney, J. Catal. 97 (1986) 390.
[26] P. Arnoldy and J.A. Moulijn, J. Catal. 93 (1985) 38.
[27] A.M. Hilmen, D. Schanke and A. Holmen, Catal. Lett. 38 (1996) 143.
[28] B. Brezny and A. Muan, J. Inorg. Nucl. Chem. 31 (1969) 649.
[29] M. Kraum and M. Baerns, Appl. Catal. A 186 (1999) 189.
[30] Y. Brik, M. Kacimi, M. Ziyad and F. Bozon-Verduraz, J. Catal. 202 (2001) 118.